CHEMISTRY
A EUROPEAN JOURNAL

DOI: 10.1002/chem.200700056

Alkaline Earth Chloride Hydrates: Chlorine Quadrupolar and Chemical Shift Tensors by Solid-State NMR Spectroscopy and Plane Wave Pseudopotential Calculations

David L. Bryce* and Elijah B. Bultz[a]

Abstract: A series of alkaline earth chloride hydrates has been studied by solid-state $^{35/37}$Cl NMR spectroscopy in order to characterize the chlorine electric field gradient (EFG) and chemical shift (CS) tensors and to relate these observables to the structure around the chloride ions. Chlorine-35/37 NMR spectra of solid powdered samples of pseudopolymorphs (hydrates) of magnesium chloride ($MgCl_2{\cdot}6H_2O$), calcium chloride ($CaCl_2{\cdot}2H_2O$), strontium chloride ($SrCl_2$, $SrCl_2{\cdot}2H_2O$, and $SrCl_2{\cdot}6H_2O$), and barium chloride ($BaCl_2{\cdot}2H_2O$) have been acquired under stationary and magic-angle spinning conditions in magnetic fields of 11.75 and 21.1 T. Powder X-ray diffraction was used as an additional tool to confirm the purity and identity of the samples. Chlorine-35 quadrupolar coupling constants (C_Q) range from essentially zero in cubic anhydrous $SrCl_2$ to 4.26 ± 0.03 MHz in calcium chloride dihydrate. CS tensor spans, Ω, are between 40 and 72 ppm, for example, $\Omega = 45 \pm 20$ ppm for $SrCl_2{\cdot}6H_2O$. Plane wave-pseudopotential density functional theory, as implemented in the CASTEP program, was employed to model the extended solid lattices of these materials for the calculation of their chlorine EFG and nuclear magnetic shielding tensors, and allowed for the assignment of the two-site chlorine NMR spectra of barium chloride dihydrate. This work builds upon our current understanding of the relationship between chlorine NMR interaction tensors and the local molecular and electronic structure, and highlights the particular sensitivity of quadrupolar nucleus solid-state NMR spectroscopy to the differences between various pseudopolymorphic structures in the case of strontium chloride.

Keywords: alkaline earth metals · chlorides · density functional calculations · hydrates · NMR spectroscopy

Introduction

The alkaline earth chlorides and their hydrates have diverse uses in chemical and industrial processes.[1] For example, calcium and magnesium chlorides are used for de-icing roads, and are also key components in the preparation of promising hydrogen storage materials which can store up to 9.1% hydrogen by weight in the form of ammonia.[2–4] Calcium chloride has been used in the development of heat storage[5] and vapor sensor materials,[6] barium chloride has been used as the basis for a humidity sensor,[7] and strontium chloride hexahydrate is used as a toothpaste additive for sensitive teeth.

[a] Prof. D. L. Bryce, E. B. Bultz
Department of Chemistry
and Centre for Catalysis Research and Innovation
University of Ottawa, Ottawa, Ontario K1N 6N5 (Canada)
Fax: (+1) 613-562-5170
E-mail: dbryce@uottawa.ca

In this work, the potential of chlorine-35/37 solid-state nuclear magnetic resonance (SSNMR)[8,9] in the characterization of alkaline earth chloride hydrates is explored. SSNMR spectroscopy is a versatile technique for studying and characterizing polymorphs and pseudopolymorphs.[10–14] NMR studies of a quadrupolar nucleus such as ^{35}Cl in the solid state can in principle yield information on the chemical shift (CS) tensor, rather than simply the isotropic chemical shift, as well as information on the electric field gradient tensor (EFG) surrounding the nucleus. The EFG tensor is directly related to the nuclear quadrupolar coupling tensor. Both the EFG and CS tensors are sensitive reporters on the local molecular and electronic structure, and as such $^{35/37}$Cl SSNMR is a potentially valuable tool for the characterization of inorganic chloride compounds.

Previous $^{35/37}$Cl NMR studies of solid inorganic chlorides are limited.[8] Stebbins and co-workers have discussed the role of chlorine NMR spectroscopy in studying chloride-containing silicate and aluminosilicate glasses;[15,16] the isotropic chlorine chemical shifts and quadrupolar parameters were

reported for anhydrous calcium chloride[15] and anhydrous barium chloride.[16] Saito has also published a ^{35}Cl magic-angle-spinning (MAS) NMR spectrum of $CaCl_2$ in an unspecified hydration state; however, no analysis of this spectrum was attempted.[17] Studies of chloride ions interacting with alkaline earth cations such as calcium are also relevant from the perspective of cement chemistry.[18–20] Chemically bound chloride ions in cements frequently exist as Friedel's salt, $Ca_2Al(OH)_6Cl{\cdot}2H_2O$, which has been studied by ^{27}Al solid-state NMR[21] as well as preliminarily by ^{35}Cl solid-state NMR.[22] Additionally, Skibsted and Jakobsen have presented a beautiful chlorine SSNMR study of quadrupolar effects in inorganic perchlorate salts.[23]

Lefebvre[24] has reported a chlorine-35/37 NMR investigation of solid alkaline earth chlorides; however, there are problems evident with the processing and interpretation of these data. Furthermore, no information was extracted on the chlorine quadrupolar coupling constant (C_Q), asymmetry parameter (η_Q), or CS tensors. Here, we present a comprehensive $^{35/37}$Cl solid-state NMR spectroscopic study of several alkaline earth chloride hydrates: $MgCl_2{\cdot}6H_2O$, $CaCl_2{\cdot}2H_2O$, $SrCl_2$, $SrCl_2{\cdot}2H_2O$, $SrCl_2{\cdot}6H_2O$, and $BaCl_2{\cdot}2H_2O$ (Figure 1). The objective is to provide accurate and precise characterization of the chlorine quadrupolar and CS tensors, and their relative orientations, and to interpret the results in terms of known diffraction-based structures (Table 1). Our recent chlorine-35/37 NMR investigations of solid amino acid hydrochlorides reveal that the chlorine chemical shift tensor spans (Ω) in these compounds are generally less than 100 ppm, with the value for L-phenylalanine hydrochloride being the largest reported to date, 129 ± 20 ppm.[25,26] For this reason, we anticipate that particularly high magnetic field strengths will be required to extract the CS tensor information for the alkaline earth chloride hydrates. Data at 11.75 and 21.1 T were therefore acquired in the present work.

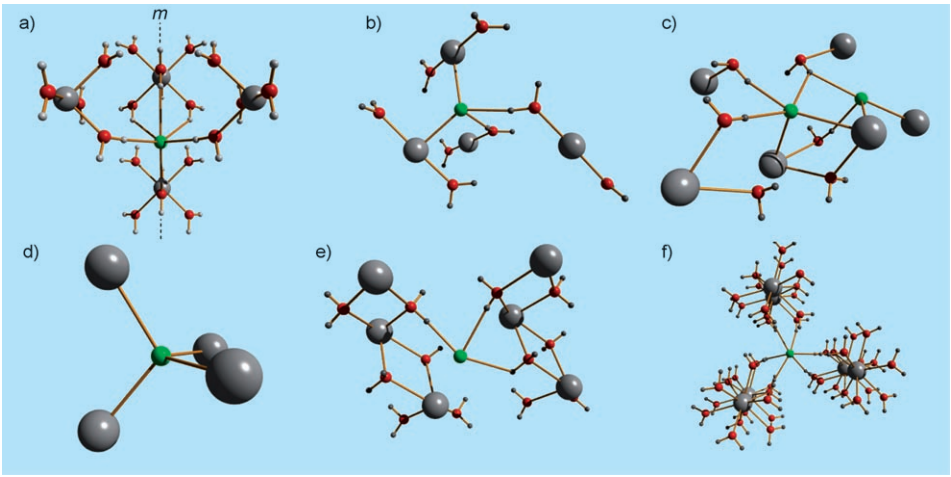

Figure 1. Local coordination environments of the chloride ions in the alkaline earth chloride pseudopolymorphs studied in this work (from diffraction studies; references are given in the text). a) $MgCl_2{\cdot}6H_2O$, b) $CaCl_2{\cdot}2H_2O$, c) $BaCl_2{\cdot}2H_2O$, d) $SrCl_2$ (anhydrous), e) $SrCl_2{\cdot}2H_2O$, f) $SrCl_2{\cdot}6H_2O$. Chlorine is shown in green; alkaline earth cations are shown in dark grey; oxygen is shown in red; hydrogen is shown in light grey. The chloride ion lies on a mirror plane, denoted "*m*" in $MgCl_2{\cdot}6H_2O$. There are two non-equivalent chlorine sites in $BaCl_2{\cdot}2H_2O$. The chloride ion lies along a C_3 rotation axis in $SrCl_2{\cdot}6H_2O$. Anhydrous $SrCl_2$ exists in a cubic structure; the four nearest-neighbor Sr atoms are shown in d). Figure prepared using Diamond 3.0[67] and PovRay 3.6.[68]

Table 1. Selected crystallographic properties of the alkaline earth chloride hydrates discussed in this study.

	Structure type	Space group	Number of unique chlorides	Cl on symmetry element?	Ref.
$MgCl_2{\cdot}6H_2O$	monoclinic	*C*2/*m*	1	Cl on mirror plane	[69]
$CaCl_2{\cdot}2H_2O$	orthorhombic	*Pbcn*	1	no	[70]
$SrCl_2$	cubic (fluorite)	*Fm*3*m*	1	yes	[71]
$SrCl_2{\cdot}2H_2O$	monoclinic	*C*2/*c*	1	no	[72]
$SrCl_2{\cdot}6H_2O$	trigonal	*P*321	1	Cl on C_3 axis	[73]
$BaCl_2{\cdot}2H_2O$	monoclinic	$P2_1/n$	2	no	[74,75]

To complement the experimental data and to aid in its interpretation, density-functional theory (DFT) calculations of the chlorine NMR interaction tensors were also carried out. Since the alkaline earth chloride hydrates form extended three-dimensional lattices in the solid state, a method implemented in the CASTEP program[27–29] which uses periodic boundary conditions to describe crystalline materials was explored. This method, which uses pseudopotentials and plane wave basis sets to describe the system,[30] has gained popularity recently for the calculation of SSNMR parameters.[13,31–38]

Results and Discussion

The experimental chlorine NMR parameters derived from this study are summarized in Table 2. Analyses of chlorine NMR spectra for each compound, in the context of their solid-state structures, are presented below.

Strontium chloride dihydrate: The structure of $SrCl_2{\cdot}2D_2O$, as refined by neutron powder diffraction at 300 K (space group *C*2/*c*), indicates that there is a single chloride ion in the asymmetric unit and that it is neither on a rotation axis nor a mirror plane (Figure 1).[72] This is consistent with earlier reports on the dihydrate.[39] Powder X-ray diffraction measurements confirm the identity of the sample used in the present work (Figure 2). The chlorine NMR interaction tensors therefore are not restricted to be axially symmetric or to have a particular orientation in the molecular frame-

Table 2. $^{35/37}$Cl Quadrupolar and chemical shift tensor parameters for some alkaline earth chlorides and their hydrates.

compound	$\lvert C_Q(^{35}Cl)\rvert$/ MHz	$\lvert C_Q(^{37}Cl)\rvert$/ MHz	η_Q	$\delta_{iso}(^{35}Cl)$/ ppm[a]	Ω/ ppm[b]	κ[c]	α, β, γ[d]/°	Ref.
$MgCl_2{\cdot}6H_2O$	3.02 ± 0.05	2.36 ± 0.02	0.0	75.0 ± 1.0	<75	–	–	this work
$CaCl_2$ (anhydrous)	2.1 ± 0.1	n.a.	0.7 ± 0.1	168 ± 5	n.a.	n.a.	n.a.	Sandland et al.[15]
$CaCl_2{\cdot}2H_2O$	4.26 ± 0.03	3.35 ± 0.03	0.75 ± 0.03	110.0 ± 2.0	72 ± 15	0.60 ± 0.20	$90\pm10, 82\pm5, 0\pm20$	this work
$SrCl_2$ (anhydrous)	≈0[e]	≈0	n.a.	188.2 ± 1.0	0.0	n.a.	n.a.	this work
$SrCl_2{\cdot}2H_2O$	1.41 ± 0.02	1.11 ± 0.02	0.80 ± 0.10	142.1 ± 1.0	41 ± 10	0.50 ± 0.20	$86\pm15, 75\pm5, 37\pm10$	this work
$SrCl_2{\cdot}6H_2O$	3.91 ± 0.05	3.05 ± 0.05	0.0	90.4 ± 1.0	45 ± 20	-1.0	$0\pm10, 90\pm10, 0\pm10$	this work
$BaCl_2$ (anhydrous; site A)	3.5 ± 0.1	n.a.	0.15 ± 0.05	124 ± 5	n.a.	n.a.	n.a.	Stebbins and Du[16]
$BaCl_2$ (anhydrous; site B)	3.95 ± 0.1	n.a.	0.1 ± 0.1	265 ± 5	n.a.	n.a.	n.a.	Stebbins and Du[16]
$BaCl_2{\cdot}2H_2O$ (site A)	2.19 ± 0.08	1.73 ± 0.08	0.0	163.4 ± 2.0	50 ± 25	-0.80 ± 0.20	$85\pm20, 32\pm10, 60\pm20$	this work
$BaCl_2{\cdot}2H_2O$ (site B)	3.42 ± 0.08	2.69 ± 0.08	0.31 ± 0.10	156.6 ± 2.0	50 ± 25	0.20 ± 0.25	$20\pm15, 8\pm10, 0\pm20$	this work

[a] Isotropic chemical shifts ($\delta_{iso}=(\delta_{11}+\delta_{22}+\delta_{33})/3$) are with respect to the ^{35}Cl central transition center band for solid powdered NaCl. [b] The chemical shift tensor span, Ω, is $\delta_{11}-\delta_{33}$ where the principal components of the CS tensor are ordered $\delta_{11}\geq\delta_{22}\geq\delta_{33}$. [c] The chemical shift tensor skew, κ, is given by $3(\delta_{22}-\delta_{iso})/\Omega$, and has allowed values between -1 and $+1$. [d] The Euler angles α, β, and γ, describe the counterclockwise rotations required to bring the EFG tensor PAS into coincidence with the CS tensor PAS. [e] Based on central transition 2nd-order quadrupolar lineshape.

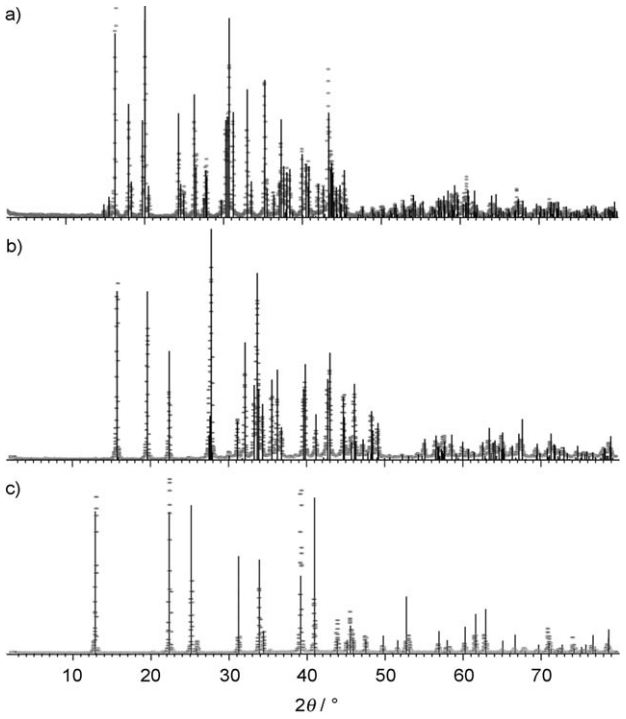

Figure 2. Experimental (·····) and theoretical (——) powder X-ray diffraction ($Cu_{K\alpha1}$ radiation) patterns for a) barium chloride dihydrate, b) strontium chloride dihydrate, and c) strontium chloride hexahydrate. Discrepancies between some of the predicted and experimental intensities are attributed to preferential alignment of certain crystallites, and are not related to phase purity.

work. Shown in Figure 3 is a series of chlorine solid-state NMR spectra obtained for $SrCl_2{\cdot}2H_2O$. Chlorine-35 MAS NMR spectra were recorded at 21.1 and 11.75 T, and a chlorine-37 MAS NMR spectrum was recorded at 11.75 T. Simulations of these spectra provided the quadrupolar parameters and the isotropic chemical shift given in Table 2. The value of $\lvert C_Q(^{35}Cl)\rvert$, 1.41 ± 0.02 MHz, is small relative to the other alkaline earth chloride hydrates, but comparable to the values reported by Honda for *n*-alkylammonium chlorides.[40] The value of $\lvert C_Q(^{37}Cl)\rvert$ determined directly from the ^{37}Cl MAS NMR spectrum, 1.11 ± 0.02 MHz, is identical to the value predicted from the product of $\lvert C_Q(^{35}Cl)\rvert$ and the ratio of the nuclear electric quadrupole moments (Q) for the two chlorine isotopes ($Q(^{37}Cl)/Q(^{35}Cl)=0.7881$).[41] As suggested by the diffraction-based structures, the EFG tensor is not axially symmetric; the combined analysis of the ^{35}Cl and ^{37}Cl MAS NMR spectra provide a value for the quadrupolar asymmetry parameter, η_Q, of 0.80 ± 0.10 (where $\eta_Q=(V_{11}-V_{22})/V_{33}$ and the principal components of the EFG tensor are ordered as follows: $\lvert V_{33}\rvert\geq\lvert V_{22}\rvert\geq\lvert V_{11}\rvert$).

NMR spectra of stationary samples of $SrCl_2{\cdot}2H_2O$ were obtained at 21.1 (^{35}Cl) and 11.75 T ($^{35/37}$Cl) (Figure 3). These spectra reflect the magnitude of the CS tensor, the magnitude of the EFG tensor, and the relative orientations of these two tensors. Having determined the EFG tensor magnitude and isotropic chemical shift from the spectra of MAS samples, simulations of the spectra of stationary samples yield in addition the CS tensor parameters given in Table 2. The span (Ω) of the CS tensors:

$$\Omega = \delta_{11}-\delta_{33} \quad (1)$$

(where the principal components of the CS tensor are denoted as $\delta_{11}\geq\delta_{22}\geq\delta_{33}$), is found to be 41 ± 10 ppm. The CS tensor is not axially symmetric, which is again consistent with the crystal symmetry. Finally, the Euler angles relating the chlorine EFG and CS tensors also indicate that there is no symmetry element enforcing a particular relative orientation (Table 2). To demonstrate the pronounced effect of the anisotropy of the CS tensor on the chlorine-35/37 NMR spectra, simulated spectra which incorporate an isotropic CS tensor ($\Omega=0$) are also displayed in Figure 3e,j,o).

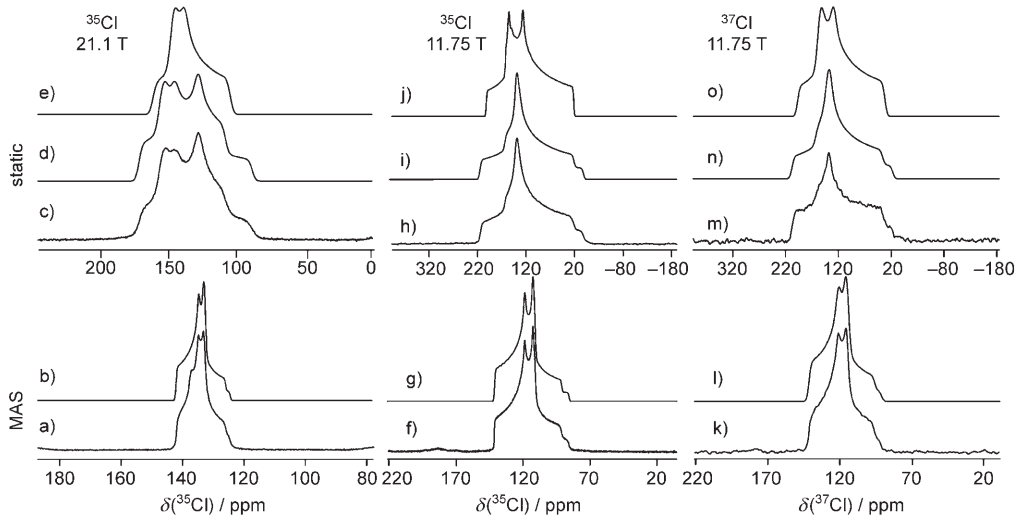

Figure 3. $^{35/37}$Cl NMR of solid powdered $SrCl_2{\cdot}2H_2O$. a), f) ^{35}Cl spectra of a MAS sample obtained at 21.1 and 11.75 T, respectively. Best-fit simulated spectra are shown in b) and g). k) ^{37}Cl spectrum of a MAS sample obtained at 11.75 T. The best-fit simulated spectrum is shown in l). c), h) ^{35}Cl spectra of a stationary powdered sample obtained at 21.1 and 11.75 T, respectively. The corresponding best-fit simulated spectra are shown in d) and i). The span of the CS tensor is set to zero in e) and j) to demonstrate the large effect that anisotropy of the CS tensor has on the spectrum. m) ^{37}Cl spectrum of a stationary powdered sample obtained at 11.75 T. The best-fit simulated spectrum is shown in n), and a simulated spectrum for which the CS tensor span is set to zero is shown in o).

Strontium chloride hexahydrate: A single-crystal neutron diffraction structure of strontium chloride hexahydrate at room temperature (space group *P*321) reveals a single chloride ion in the asymmetric unit.[73] The structure is consistent with earlier X-ray diffraction studies,[42] and is isotypal with calcium chloride hexahydrate[73] as well as strontium bromide hexahydrate.[43] The chloride sits on a threefold rotation axis which dictates that its NMR interaction tensors must have axial symmetry, with the unique principal axis for each tensor lying along the C_3 axis. The ^{35}Cl MAS NMR spectrum acquired at 21.1 T indeed exhibits a second-order central-transition (CT) quadrupolar lineshape corresponding to an axially symmetric EFG tensor (Figure 4). The value of $|C_Q(^{35}Cl)|$, 3.91 ± 0.05 MHz, results from fitting MAS NMR spectra obtained at 11.75 and 21.1 T. Since the trace of the EFG tensor is zero ($V_{33} + V_{22} + V_{11} = 0$), and the chlorine EFG tensor for $SrCl_2{\cdot}6H_2O$ is axially symmetric ($V_{11} = V_{22}$) we may conclude that the largest component, V_{33}, lies along the C_3 axis. In terms of the local molecular structure, V_{33} is directed along the axis on which all the chloride ions lie (i.e., the axis which is perpendicular to the plane of Figure 1f).

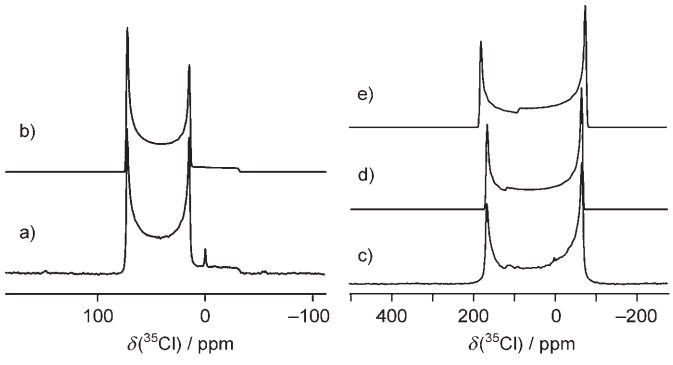

Figure 4. ^{35}Cl NMR spectra of solid $SrCl_2{\cdot}6H_2O$. a) Spectrum of a MAS sample ($\nu_{rot} = 18$ kHz), obtained at 21.1 T. The best-fit simulation is shown in b). A trace impurity of NaCl(s) is seen at 0 ppm. c) Spectrum of a stationary sample obtained at 21.1 T. The best-fit simulation is shown in d). A spectrum simulated with a span of 0 ppm is shown in e) for comparison. Parameters used in the simulations are given in Table 2.

A ^{35}Cl NMR spectrum of a stationary powdered sample of strontium chloride hexahydrate obtained at 21.1 T can only be properly reproduced when a CS tensor with a span of 45 ± 20 ppm is included in the simulation (Figure 4). This chlorine CS tensor span is comparable to those obtained for a variety of amino acid hydrochlorides.[25,26] Due to the C_3 symmetry axis passing through chlorine, the skew ($\kappa = 3(\delta_{22} - \delta_{iso})/\Omega$) of the CS tensor must be ± 1.0 and the Euler angles (α, β, γ) describing the relative orientations of the EFG and CS tensors are restricted to possibilities which place one of the principal axes of the CS tensor coincident with V_{33}. The known crystal symmetry therefore helps greatly in narrowing down the parameter space to be searched during spectral simulation. We find that the only possibility which results in a spectral simulation in complete agreement with the experimental spectrum is $\kappa = -1.0$ and $\alpha = 0$, $\beta = 90$, $\gamma = 0°$. Physically, this corresponds to colinearity of V_{33} and the most deshielded principal component (δ_{11}) of the CS tensor.

In some cases, a conversion of $SrCl_2{\cdot}6H_2O$ to $SrCl_2{\cdot}2H_2O$ through an unknown intermediate hydrate form was observed under MAS conditions (Figure 5). This dehydration is most likely due to the frictional heating which occurs

during MAS.[44–47] For example, it was recently shown that the polymorphic product distribution in the solid-state dehydration of sodium acetate trihydrate was altered by carrying out this process under high-speed MAS conditions.[48] At present, it is not entirely clear what factors control the present conversion of $SrCl_2{\cdot}6H_2O$ to $SrCl_2{\cdot}2H_2O$, since clean MAS spectra of the hexahydrate were also obtained in some cases (see above, Figure 4). The example presented in Figure 5 demonstrates the utility of solid-state chlorine-35/37 NMR spectroscopy in the identification and differentiation of different inorganic pseudopolymorphs. When compared, in addition, to the spectral signature of anhydrous strontium chloride (Figure 5), it is remarkable that three different pseudopolymorph chlorine NMR lineshapes are well-resolved and identifiable at 11.75 T.

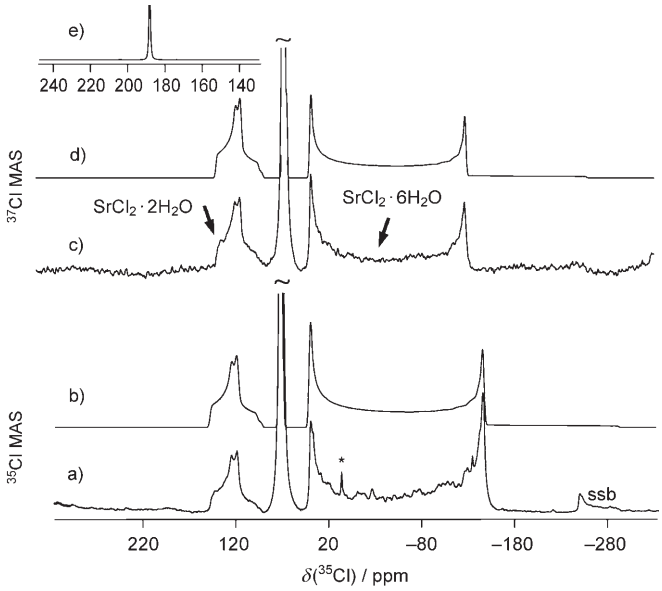

Figure 5. $^{35/37}$Cl MAS NMR spectra obtained at 11.75 T of mixtures of strontium chloride hydrate pseudopolymorphs generated in situ during the experiment. Experimental spectra are shown in a) ^{35}Cl and c) ^{37}Cl, with best-fit simulations shown in b) and d). $SrCl_2{\cdot}2H_2O$ appears on the high-frequency side of the spectra (cf. Figure 3) and $SrCl_2{\cdot}6H_2O$ appears on the low-frequency side (cf. Figure 4). The relatively sharp peak at $\approx$68 ppm likely corresponds to a third pseudopolymorphic form. A trace amount of NaCl(s) is denoted by an asterisk in a). e) ^{35}Cl MAS NMR spectrum of a separately prepared sample of anhydrous $SrCl_2$.

Anhydrous strontium chloride: Dry $SrCl_2$ is known to crystallize in the cubic fluorite-type structure.[71] Bowers and Mueller have presented a ^{87}Sr SSNMR study of this compound and suggested that solid strontium chloride has a relatively small number of site defects which would cause the EFG at Sr to deviate from exactly zero.[49] Consistent with these findings and with the known cubic structure, a sharp ^{35}Cl CT lineshape devoid of 2nd-order quadrupolar effects was observed under MAS conditions for dry $SrCl_2$ (Figure 5e). The isotropic ^{35}Cl chemical shift is therefore taken to be the center-of-gravity of this resonance, 188.2 ± 1.0 ppm with respect to solid sodium chloride.

Calcium chloride dihydrate: $CaCl_2{\cdot}2H_2O$ crystallizes in the space group *Pbcn* and there is a single chloride site in the asymmetric unit.[70] This chloride ion is neither on a rotation axis nor a mirror plane and therefore axial symmetry of the EFG and CS tensors is not anticipated, nor is any coincidence in the orientations of the principal axis systems of these tensors.

Simulation of a ^{35}Cl MAS NMR spectrum of calcium chloride dihydrate acquired at 21.1 T (Figure 6f) affords the ^{35}Cl quadrupolar coupling constant, $\pm(4.26 \pm 0.03$ MHz), which is the largest known for the alkaline earth chloride polymorphs and hydrates. The observed value of η_Q, 0.75 ± 0.03, is consistent with the diffraction data which do not place the chloride ion on a symmetry element. The quadrupolar parameters, as well as the isotropic chemical shift of 110.0 ± 2.0 ppm, are significantly different from those reported by Sandland et al. for anhydrous $CaCl_2$ (Table 2).[15] This speaks to the sensitivity of the chlorine NMR parameters to subtle but important differences in the hydration state of the sample.

Also shown in Figure 6 is the ^{35}Cl NMR spectrum of a stationary sample of $CaCl_2{\cdot}2H_2O$ acquired at 21.1 T, and the best-fit simulation (Figure 6c,d). A low-frequency splitting

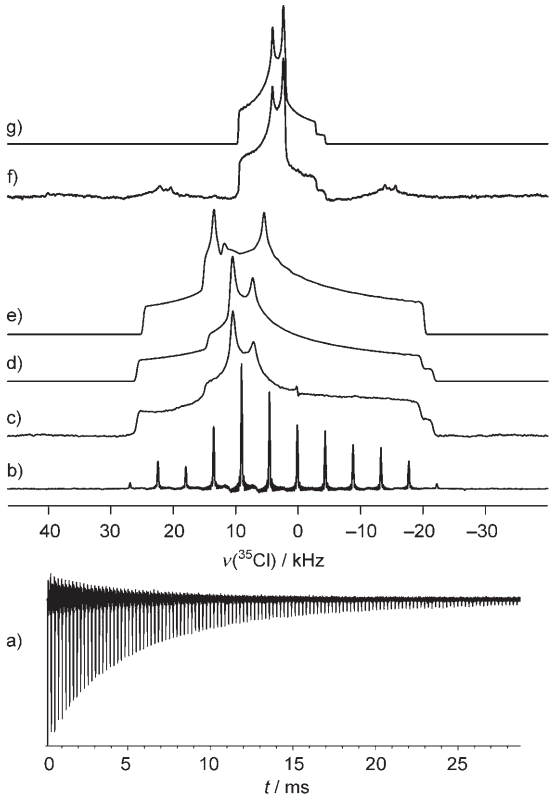

Figure 6. ^{35}Cl NMR of solid powdered $CaCl_2{\cdot}2H_2O$ at 21.1 T. a) QCPMG FID echo train; the FT spectrum is shown in b). Shown in c) is the ^{35}Cl spin-echo spectrum acquired under stationary conditions. The corresponding best-fit simulated spectrum is shown in d). For comparison, a simulated spectrum which was generated under the assumption of an isotropic CS tensor is presented in e). Shown in f) is the MAS ^{35}Cl NMR spectrum obtained at an MAS rate of 18 kHz. The simulated spectrum is shown in g).

of the shoulder of the spectrum is an important feature which indicates significant chlorine CS anisotropy. Indeed, a simulated spectrum which incorporates only quadrupolar effects (Figure 6e) demonstrates the significant impact of the CS tensor on the high-field chlorine NMR spectrum. To maximize the accuracy and precision with which the CS tensor parameters are determined, the 21.1 T spectrum was fit simultaneously with ^{35}Cl and ^{37}Cl NMR spectra of a stationary sample acquired at 11.75 T (Figure 7). The effects of chemical shift anisotropy, while more subtle at 11.75 T, are still evident (Figure 7c,d). The non-axial symmetry of the CS

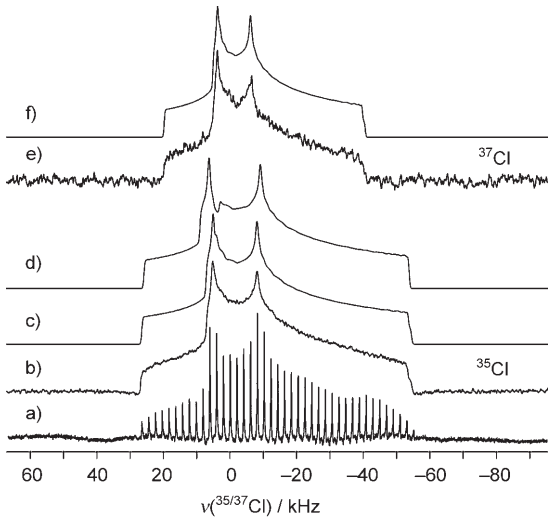

Figure 7. a) ^{35}Cl QCPMG and b) quadrupolar echo and e) ^{37}Cl quadrupolar-echo NMR spectra of powdered $CaCl_2{\cdot}2H_2O$ acquired at 11.75 T under stationary conditions. Shown in c) and f) are the corresponding best-fit simulated spectra based on the parameters given in Table 2. For comparison, shown in d) is the simulated ^{35}Cl NMR spectrum obtained when the chemical shift tensor is assumed to be isotropic ($\Omega = 0$).

tensor ($\kappa = 0.60 \pm 0.20$) is again consistent with the lack of crystallographic symmetry at chlorine. The span of the CS tensor, 72 ± 15 ppm, is the largest measured amongst the alkaline earth chloride hydrates (Table 2). This value is intermediate with respect to the range of all experimentally known chlorine CS tensor spans,[8,25,26] and significantly larger than previously reported spans for inorganic chlorides.[50]

Calcium chloride dihydrate proved to be an excellent sample for ^{35}Cl QCPMG NMR experiments as shown in Figures 6b and 7a. The NMR signal can continue to be refocused for longer than 30 ms as depicted in Figure 6a. Given the commercial availability of $CaCl_2{\cdot}2H_2O$, this sample would be useful for setting up QCPMG NMR experiments for future $^{35/37}$Cl SSNMR studies.

Barium chloride dihydrate: The crystal structure of $BaCl_2{\cdot}2H_2O$ has been determined by neutron diffraction.[74,75] The compound crystallizes in the space group $P2_1/n$ and there are two crystallographically distinct chloride ions in the asymmetric unit (sites 1 and 2). This has also been seen in electron diffraction studies.[51] The observed powder X-ray diffraction pattern for the sample used in the present study is consistent with the neutron diffraction structure (Figure 2). The ^{35}Cl and ^{37}Cl MAS NMR spectra of $BaCl_2{\cdot}2H_2O$ reveal two distinct second-order CT quadrupolar lineshapes (Figure 8), which each correspond to one of the two sites identified in the neutron diffraction study. Neither chloride is on a rotation axis, inversion center, or mirror plane. As such, there is no symmetry element enforcing axial symmetry or absolute or relative orientations of the chlorine NMR interaction tensors. One of the two sites in the NMR spectrum (which we label A and B) has an associated quadrupolar asymmetry parameter of 0.31 ± 0.10, while the other exhibits an axially symmetric ($\eta_Q = 0.00$) lineshape, despite the fact that there is no local symmetry element which absolutely requires this. On the basis of the experimental NMR data alone, it is therefore difficult to assign the two spectral signatures specifically to the two crystallographic sites. DFT calculations were used to aid in the assignment (see below). The chlorine quadrupolar coupling constants ($|C_Q(^{35}\mathrm{Cl})| = 2.19 \pm 0.08$ and 3.42 ± 0.08 MHz; $|C_Q(^{37}\mathrm{Cl})| = 1.73 \pm 0.08$ and 2.69 ± 0.08 MHz) and isotropic chemical shifts (163.4 ± 2.0 and 156.6 ± 2.0 ppm) determined from the MAS NMR spectra are significantly different for sites A and B, indicating the utility of chlorine-35/37 SSNMR in the clear differentiation of crystallographically non-equivalent (but chemically identical) chloride sites in inorganic materials.

The quadrupolar and isotropic chemical shift data obtained for $BaCl_2{\cdot}2H_2O$ may be compared with data reported for the anhydrous orthorhombic form[52] by Stebbins and Du.[16] As depicted in Figure 1, the chloride ions in the dihydrate interact with water protons in addition to barium cations. These extra opportunities for hydrogen bonding to chloride, and the concomitant increase in local symmetry at chloride, may in part explain why the chlorine quadrupolar coupling constants are slightly higher in the anhydrous form than in the dihydrate (see Table 2). In any event, it is gratifying to see that all four chloride sites (two in the dihydrate and two in the anhydrous form) give rise to distinct second-order CT lineshapes and isotropic chemical shifts; this shows the sensitivity of the chlorine EFG and CS tensors to the local chloride environment, and bodes well for further NMR studies of crystalline and amorphous chloride-containing materials.

Having determined the $^{35/37}$Cl quadrupolar parameters from the MAS NMR spectra of $BaCl_2{\cdot}2H_2O$, spectra of stationary samples were acquired and simulated to extract the CS tensor parameters and the Euler angles relating the EFG and CS tensor orientations (Figure 8). The CS tensor spans, 50 ± 25 ppm, are comparable to those measured for the strontium chloride hydrates. Given that there are two overlapping sites in the spectrum, relatively large errors were assigned to the span, the skew, and the angular parameters (Table 2). Nevertheless, there are some clear-cut spectral features, particularly at 21.1 T, which can only be properly simulated with a narrow range of parameters. Further-

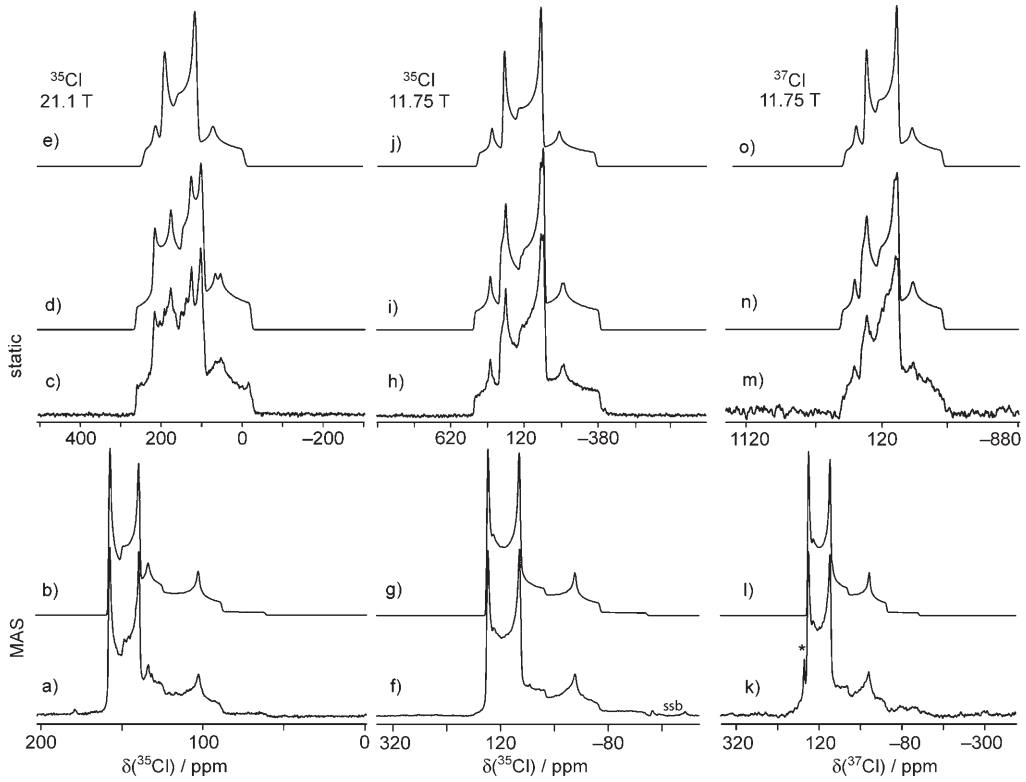

Figure 8. $^{35/37}$Cl NMR spectra of solid $BaCl_2{\cdot}2H_2O$ obtained at 11.75 and 21.1 T. a), f) ^{35}Cl MAS NMR spectra obtained at 21.1 and 11.75 T, respectively. Best-fit simulated spectra are shown in b) and g). k) ^{37}Cl MAS NMR spectrum obtained at 11.75 T; the best-fit simulation is shown in l). c), h) ^{35}Cl NMR spectra of stationary powdered samples obtained at 21.1 and 11.75 T, respectively. Best-fit simulations are shown in d) and i). m) ^{37}Cl NMR spectrum of a stationary powdered sample obtained at 11.75 T; the best-fit simulation is shown in n). All simulations are based on the parameters given in Table 2. For comparison, spectra of stationary samples have been simulated with the span of the CS tensor set to zero (see parts e, j, and o) to demonstrate the importance of the chemical shift tensor in obtaining accurate fits.

more, the availability of data acquired two magnetic field strengths, and for two chlorine isotopes is key to achieving the accurate and precise data reported in Table 2.

Magnesium chloride hexahydrate: The single-crystal neutron diffraction structure for $MgCl_2{\cdot}6H_2O$ (monoclinic, space group $C2/m$) indicates that there is a single chloride in the asymmetric unit.[69] This chloride ion lies on a mirror plane thereby dictating that one of the principal components of the EFG tensor (V_{33}) and one of the principal components of the CS tensor must be coincident and perpendicular to this plane. Presented in Figure 9 are the ^{35}Cl and ^{37}Cl NMR spectra of a MAS sample of magnesium chloride hexahydrate. The quadrupolar asymmetry parameter of zero is in agreement with the crystal symmetry. Attempts to record $^{35/37}$Cl NMR spectra of a stationary sample of hygroscopic $MgCl_2{\cdot}6H_2O$ invariably revealed more than one hydrate or polymorph in the sample. It is likely that the longer acquisition times required for obtaining good quality spectra of stationary samples allowed this interconversion of hydration states to occur, while MAS NMR spectra representative of a single phase were often obtained (Figure 9). Nevertheless, an upper limit on the span of the chlorine CS tensor of 75 ppm could be estimated from the spectra of stationary samples (not shown).

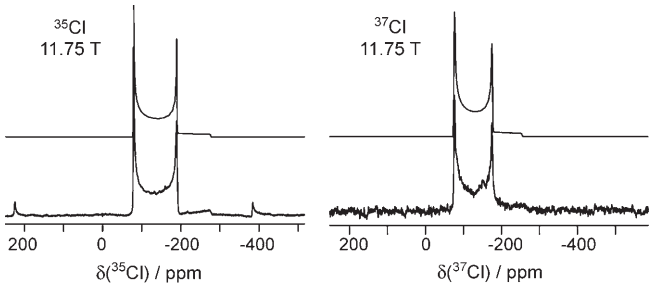

Figure 9. ^{35}Cl (left) and ^{37}Cl (right) NMR spectra of solid $MgCl_2{\cdot}6H_2O$ undergoing MAS at 15 kHz. Experimental spectra are shown in the lower traces and simulated spectra are shown in the upper traces. First-order spinning sidebands are evident in the experimental ^{35}Cl NMR spectrum.

Plane-wave calculations of the chlorine NMR interaction tensors: Shown in Table 3 are the results of CASTEP NMR plane-wave pseudopotential DFT calculations of the chlorine EFG and nuclear magnetic shielding tensors for the alkaline earth chloride hydrates studied experimentally. This type of calculation, which uses periodic boundary conditions to model the extended solid lattice, is ideal for the alkaline earth chloride hydrates which form inherently extended three dimensional networks in the solid state.[27,30] It is very

Table 3. CASTEP plane-wave calculations of the chlorine electric field gradient and nuclear magnetic shielding tensors for some alkaline earth chloride hydrates.[a]

compound	$C_Q(^{35}Cl)$/MHz	η_Q	σ_{iso}/ppm	δ_{iso}/ppm[b]	Ω/ppm	κ
$MgCl_2{\cdot}6H_2O$	−3.92	0.01	925.0	94.4	59.0	0.52
$CaCl_2{\cdot}2H_2O$	6.69	0.04	820.1	199.3	141.4	0.36
$SrCl_2{\cdot}2H_2O$	−2.00	0.59	811.0	208.4	60.5	0.23
$SrCl_2{\cdot}6H_2O$	4.95	0.00	903.2	116.2	53.8	−1.0
$BaCl_2{\cdot}2H_2O$ (site 1)	−2.43	0.07	797.0	222.4	86.3	−0.47
$BaCl_2{\cdot}2H_2O$ (site 2)	−4.96	0.30	805.3	214.1	49.2	−0.17

[a] Computed with the PBE functional and a plane wave basis set. See "Experimental and Computational Details" for further information. [b] Chemical shifts are with respect to the ^{35}Cl CT center band of solid NaCl. They are determined from the calculated magnetic shielding constants according to the following relations: i) δ_{iso}(wrt NaCl(aq)) = 974 ppm − σ_{iso}; ii) δ_{iso}(wrt NaCl(s)) = δ_{iso}(wrt NaCl(aq)) + 45.4 ppm.

difficult to build a suitable "molecular" model system for these networks.

The computational results reproduce, to varying degrees, the experimental trends in nuclear quadrupolar coupling constants, isotropic chemical shifts, and anisotropic properties of the shielding tensor (Figure 10). In particular, the theoretical trend in $C_Q(^{35}Cl)$ agrees very well with that observed experimentally (Pearson's correlation coefficient $R=0.995$). Furthermore, the calculations provide the signs of the quadrupolar coupling constants, which are not available from the current experimental study. The line of best-fit (C_Q(calcd)/MHz = 1.3941(C_Q(exptl)/MHz) + 0.1562 MHz), however, indicates a significant and consistent overestimation of the magnitude of C_Q by the calculations. A similar systematic overestimation of $C_Q(^{35}Cl)$ by plane wave-pseudopotential calculations relative to experiment has been reported by Gervais et al. for L-tyrosine hydrochloride, glycine hydrochloride, L-valine hydrochloride, and L-glutamic acid hydrochloride.[53] Plane wave basis sets with higher cut-off energies may offer modest improvement in the agreement between experiment and theory; however, previous work has shown that in at least one case, calculated quadrupolar coupling constants increase moderately as the cut-off energy is increased.[29]

In the case of isotropic chemical shifts, a significant overestimation by the calculations is also seen (Figure 10b). For example, in the case of $CaCl_2{\cdot}2H_2O$, δ_{iso} is predicted to be 199.4 ppm by the calculations whereas the experimental value is 110 ± 2 ppm (wrt solid NaCl). Further investigation shows that all principal components of the CS tensor are overestimated, and that the discrepancy is not caused by poor reproduction of a single principal component. Trends in the purely anisotropic properties of the CS tensor are difficult to compare with experiment since the experimental errors on Ω are relatively large and the total range of the observed values of Ω is small (41 ± 10 ppm for $SrCl_2{\cdot}2H_2O$ to 72 ± 15 ppm for $CaCl_2{\cdot}2H_2O$). Nevertheless, the calculated values of Ω are generally within the overall range observed experimentally. Furthermore, the compound with the largest experimental chlorine CS tensor span ($CaCl_2{\cdot}2H_2O$) also has the largest theoretical span.

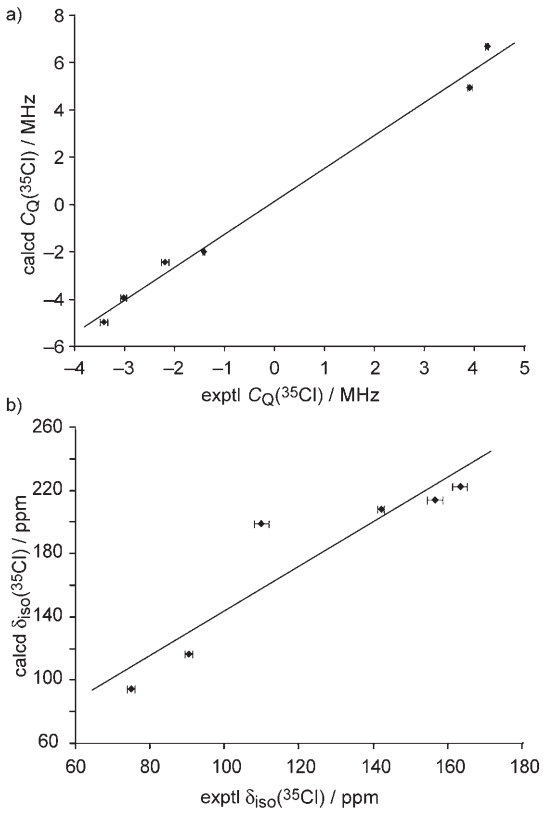

Figure 10. Calculated vs experimental chlorine NMR parameters for alkaline earth chloride hydrates. a) ^{35}Cl nuclear quadrupolar coupling constants (C_Q(calcd)/MHz = 1.3941(C_Q(exptl)/MHz) + 0.1562 MHz; $R=0.995$); b) isotropic chemical shifts (δ_{iso}(calcd)/ppm = 1.4016(δ_{iso}(exptl)/ppm) + 3.4923 ppm; $R=0.921$). DFT calculations are with the PBE functional and plane-wave basis sets. See text for further details. The "experimental" signs of the quadrupolar coupling constants are inferred from the calculations.

The plane wave calculations allow for the clear assignment of the two chlorine sites observed in the chlorine-35/37 NMR spectra of $BaCl_2{\cdot}2H_2O$ to the two sites observed in the neutron diffraction structure[75] of this compound. In the chlorine NMR spectra, site A exhibits a smaller ^{35}Cl quadrupolar coupling constant and a larger isotropic chemical shift than does site B (see Table 2). The calculations indicate that the chloride site labeled 1 in the diffraction structure[75] experiences a smaller electric field gradient and a larger chemical shift than does site 2. The measured quadrupolar asymmetry parameters (exptl: 0.0 and 0.31 for sites A and B, respectively; calcd: 0.07 and 0.30 for sites 1 and 2, respectively) also provide additional help in the assignment of the two sites. We conclude that site A corresponds to site 1 and site B corresponds to site 2. In terms of the solid-state structure, the value of η_Q which approaches zero for site 1 may be rationalized by considering that this site has three nearest-neighbor (less than 3.5 Å away) barium ions which lie *roughly* in the same plane and create approximate local C_3 symmetry around the chloride. Site 2 has only two such

nearest neighbors which cannot approximate three-fold symmetry which would cause η_Q to tend towards zero.

Conclusion

A detailed study of the chlorine NMR properties of several solid alkaline earth chloride hydrates has been presented. The results demonstrate that chlorine NMR spectroscopy has the potential to become a more widely-used tool for the characterization of solid inorganic chloride materials. The case of barium chloride dihydrate has shown the utility of the method in identifying magnetically non-equivalent chloride sites in the asymmetric unit of the crystal. The case of strontium chloride hydrates has provided an example where several different pseudopolymorphs can be identified, each of which give rise to distinct and well-resolved ^{35}Cl NMR spectral signatures. These results exemplify the fact that the chlorine quadrupolar coupling constant, asymmetry parameter, and isotropic chemical shift are all useful parameters for identifying and distinguishing between various compounds and hydrates. Figure 11 summarizes the chlorine isotropic chemical shifts which are now known for alkaline earth chlorides and their hydrates. It is clear that there is no obvious correlation between the chemical shift and for example, the identity of the central alkaline earth metal. In general terms, the more strongly hydrated species tend to have larger shielding constants. Additional studies will be helpful in further elucidating the detailed relationship between the chlorine chemical shift and local structural parameters.

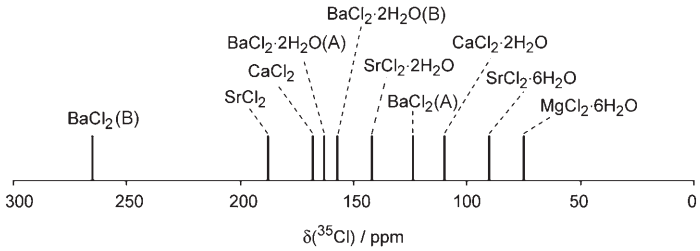

Figure 11. ^{35}Cl isotropic chemical shift scale for various alkaline earth chlorides and their hydrates (with respect to solid sodium chloride at 0 ppm). Data are from Table 2.

Of particular fundamental importance is the fact that solid-state ^{35}Cl NMR data acquired at 11.75 and 21.1 T, as well as ^{37}Cl NMR data obtained at 11.75 T have allowed for the characterization of chlorine chemical shift tensors in inorganic chloride compounds. The 21.1 T data were essential for this part of the work. To our knowledge, these results represent the most extensive study of chloride CS tensors in inorganic compounds to date. The magnitudes of the chlorine EFG and CS tensors are, on the whole, comparable to those observed previously for a series of amino acid hydrochlorides.[25,26,53,66]

Plane wave pseudopotential calculations were found to reproduce the experimental trend in chlorine quadrupolar coupling constants particularly well; however, their absolute values were consistently overestimated relative to experiment. With respect to the chemical shift tensor, all three principal components were also overestimated relative to experiment, while the span of the CS tensor was predicted with somewhat more accuracy. Further calculations as well as experimental data will be vital in establishing more general conclusions.

Experimental and Computational Details

Sample preparation and powder X-ray diffraction: $BaCl_2{\cdot}2H_2O$ was obtained from Aldrich Chemical Company. Powder X-ray diffraction confirmed the identity of the sample as being the dihydrate (see Figure 2), with the structure reported by Padmanabhan et al.[74,75] This sample was used without further purification for SSNMR experiments.

Dry $SrCl_2$ was obtained by heating a commercial sample of $SrCl_2{\cdot}6H_2O$ in an oven at 300 °C for several days. Its identity as the anhydrous form was confirmed by the sharp ^{35}Cl NMR resonance devoid of 2nd-order quadrupolar effects, consistent with the known cubic structure of $SrCl_2$.

$SrCl_2{\cdot}2H_2O$ was prepared by allowing a supersaturated aqueous solution of strontium chloride hexahydrate to form crystals above 61.5 °C.[1] Above this temperature, the dihydrate crystallizes in rectangular plates. Powder X-ray diffraction confirmed the identity of the sample as being the dihydrate (see Figure 2), with the structure reported by Möller and Lutz.[72] Anhydrous $SrCl_2$ is known to form some $SrCl_2{\cdot}2H_2O$ as it hydrates in air to finally form the hexahydrate; however, this is not a viable method for obtaining pure hydrates, since the monohydrate is also produced, as discussed by Basiev et al.[54]

$SrCl_2{\cdot}6H_2O$ was obtained from Aldrich Chemical Company. Initial powder X-ray diffraction experiments revealed this sample to be a mixture of the dihydrate and the hexahydrate. The sample was therefore recrystallized from water at room temperature to yield the pure hexahydrate (hexagonal needles).[1] Powder X-ray diffraction confirmed that the product so obtained was the hexahydrate (see Figure 2), with the structure reported by Agron and Busing.[73]

$CaCl_2{\cdot}2H_2O$ was obtained from Fisher Scientific. The commercial sample was used without further purification for SSNMR experiments; however, the same NMR spectra were obtained when the pure dihydrate was obtained upon recrystallization of the sample from water following the procedure described by Leclaire and Borel.[70] Furthermore, identical NMR spectra were obtained from a second sample of $CaCl_2{\cdot}2H_2O$ obtained from Aldrich. It was not possible to record reliable powder X-ray diffraction data for $CaCl_2{\cdot}2H_2O$ with our existing equipment due to the extremely hygroscopic nature of this sample.

$MgCl_2{\cdot}6H_2O$ was obtained from Aldrich Chemical Company. Powder X-ray diffraction confirmed the identity of the sample as the hexahydrate, with the structure reported by Agron and Busing.[69] The hexahydrate is known to be the only stable form between −3.4 and 116.7 °C.[1]

Samples were ground into fine powders with a mortar and pestle for X-ray diffraction experiments, and subsequently packed into 4.0 and 3.2 mm o.d. zirconia rotors for SSNMR experiments.

Powder X-ray diffraction data were collected using a Philips PW3719 diffractometer and $Cu_{K\alpha1}$ radiation ($\lambda = 1.54056$ Å); operating conditions were 45 kV and 40 mA. A 10 mm slit was used at the X-ray source; the scattering slit had a fixed width of 0.2 mm, and a 1° receiving slit was used. Data were collected in continuous mode over the range $2\theta = 2.01$ to 79.99° in steps of 0.02° at a rate of 1.2° per minute.

Theoretical X-ray powder diffraction patterns were generated using the published single-crystal data and the program Diamond 3.0.[67]

Solid-state NMR Spectroscopy

At 11.75 T: Chlorine-35 NMR spectra were obtained on a widebore Bruker Avance 500 spectrometer operating at a frequency of 49.0 MHz

and running XWinNMR 3.2. Chlorine-37 NMR spectra were obtained at 40.79 MHz. A Bruker 4 mm double-resonance MAS probe was used for all experiments. Typically, solid ammonium chloride was used as a set-up sample for pulse calibration and chemical shift referencing. The chlorine-35 chemical shift of the center band is 120.1 ppm with respect to the center band for solid NaCl.[55] The ^{35}Cl $\pi/2$ pulse length of 3.50 μs was scaled by one-half to yield a central-transition "solid" $\pi/2$ pulse length of 1.75 μs which was used for experiments on the alkaline earth chloride hydrates. For ^{37}Cl, the solid $\pi/2$ pulse length was 2.37 μs. Pulse-acquire or rotor-synchronized quadrupolar echo ($\pi/2 - \tau - \pi/2 - \tau -$ acquire) sequences, with proton decoupling during acquisition, were employed for MAS samples. MAS rates of 10–15 kHz were employed. For stationary samples, a quadrupolar echo ($\pi/2 - \tau - \pi/2 - \tau -$ acquire) sequence was used, or its hyperbolic secant-enhanced variant.[56] Recycle delays ranged from 2–10 s for the alkaline earth chloride hydrates. Quadrupolar Carr–Purcell–Meiboom–Gill (QCPMG) experiments[57–59] were also performed on $CaCl_2{\cdot}2H_2O$.

At 21.1 T: Chlorine-35 NMR spectra were obtained on a Bruker Avance II 900 spectrometer operating at a frequency of 88.1 MHz and running TopSpin 1.3 software. A Bruker 3.2 mm double-resonance MAS probe (serial number 0001) was used for all experiments. Solid NaCl(s) was used as a chemical shift reference (0 ppm) and for pulse calibration. Typical $\pi/2$ pulse lengths were 3.35–3.47 μs. The CT-selective $\pi/2$ pulse was therefore set at 1.68–1.74 μs. For stationary samples, an echo ($\pi/2 - \tau - \pi - \tau -$ acquire) sequence was used, with proton decoupling during acquisition. Recycle delays ranged from 2–10 s for the alkaline earth chloride hydrates. MAS rates used ranged from 10 to 18 kHz. QCPMG experiments were also performed on $CaCl_2{\cdot}2H_2O$.

Spectral processing and simulations: All spectra were apodized with an exponential window function and zero-filled to at least twice their original size prior to Fourier transformation. Spectral lineshape simulations[60] were performed with WSOLIDS1 version 1.17.30.[61] A lineshape fitting strategy was employed in which the CT center band lineshape of a fast MAS sample is first analyzed. This lineshape and its spectral position depend on C_Q, η_Q, and δ_{iso}. The NMR spectrum of a stationary sample is then analyzed while keeping these three parameters fixed. Five adjustable parameters remain: the span, the skew, and the Euler angles α, β, and γ. To maximize the accuracy and precision with which the EFG and CS tensor parameters are determined, ^{37}Cl spectra are acquired in addition to ^{35}Cl spectra, and spectra are acquired at more than one external applied magnetic field strength. These additional data are useful because the relative effects of the quadrupolar and CS interactions differ due to the different nuclear electric quadrupole moments of the two chlorine isotopes, and due to the different manners in which the quadrupolar and nuclear magnetic shielding interactions depend on B_0. Iterative lineshape fitting was performed interactively. Emphasis was placed primarily on the fitting of key spectral discontinuities and shoulders. Stack plots were prepared using DMFit.[62]

All simulations are based on the isolated spin approximation. This approximation is valid in the present study since high-power proton decoupling is used during acquisition and since any residual dipolar interactions between $^{35/37}$Cl and nearby alkaline earth nuclides are negligible. For example, the most abundant spin-active alkaline earth nuclide in the compounds studied presently is ^{137}Ba, at only 11.23 %. The shortest contact between Cl and Ba in $BaCl_2{\cdot}2H_2O$ is 3.13 Å, which results in a ^{35}Cl,^{137}Ba direct dipolar coupling constant of only 43 Hz. Direct dipolar interactions between chlorine and other alkaline earth nuclides are smaller in magnitude.

The Maryland convention[63] on nuclear magnetic shielding and CS tensors was followed, that is, the principal components of the shielding tensor are labeled and ordered as $\sigma_{33} \geq \sigma_{22} \geq \sigma_{11}$ and those of the CS tensor as $\delta_{11} \geq \delta_{22} \geq \delta_{33}$. The span, Ω, is defined as $\sigma_{33} - \sigma_{11} \approx \delta_{11} - \delta_{33}$, and the skew ($\kappa$) is given by $3(\sigma_{iso} - \sigma_{22})/\Omega \approx 3(\delta_{22} - \delta_{iso})/\Omega$.

CASTEP Calculations: CASTEP (version 3.2)[27–29] calculations were set up using the Materials Studio graphical user interface, and run on a single CPU. CASTEP is a plane wave-based density functional theory (DFT) program which is particularly well-suited to modeling the properties of extended solid-state systems. The NMR module was used for the calculation of electric field gradient tensors and nuclear magnetic shielding tensors. The Perdew Burke Ernzerhof (PBE) functional was used within the Generalized Gradient Approximation (GGA) for all calculations.[64] Basis set cut-off energies were 550 eV ($CaCl_2{\cdot}2H_2O$; $SrCl_2{\cdot}2H_2O$; $SrCl_2{\cdot}6H_2O$; EFG tensor for $MgCl_2{\cdot}6H_2O$) or 450 eV ($BaCl_2{\cdot}2H_2O$; shielding tensor for $MgCl_2{\cdot}6H_2O$). Higher level computations were not currently possible with our available computational resources. Other computational options and convergence criteria were left at their default values. Unit cell parameters and atomic coordinates were taken from the available diffraction-based structures for $CaCl_2{\cdot}2H_2O$,[70] $BaCl_2{\cdot}2H_2O$,[74,75] $MgCl_2{\cdot}6H_2O$,[69] $SrCl_2{\cdot}2H_2O$,[72] and $SrCl_2{\cdot}6H_2O$.[73]

Chlorine-35 nuclear quadrupolar coupling constants ($C_Q = eV_{33}Q/h$, where e is the fundamental electric charge, V_{33} is the EFG tensor eigenvalue of the largest absolute value, Q is the nuclear electric quadrupole moment, and h is Planck's constant) and quadrupolar asymmetry parameters ($\eta_Q = (V_{11} - V_{22})/V_{33}$), where the principal components of the EFG tensor are ordered $|V_{33}| \geq |V_{22}| \geq |V_{11}|$) were calculated automatically from the EFG tensor by CASTEP. Values of C_Q produced by CASTEP were subsequently rescaled so that the recommended value[41] of the ^{35}Cl nuclear electric quadrupole moment, −81.65 mb, is used rather than −81.10 mb (the default value used by CASTEP).

The isotropic chemical shifts and chemical shift tensor eigenvalues were determined using the calculated chlorine magnetic shielding tensors and the absolute shielding scale for chlorine:[65]

$$\delta_{ii} = 974\,\text{ppm} - \sigma_{ii} \quad (2)$$

where $ii = 11$, 22, 33, or "iso" and where 974 ppm is the absolute shielding constant for the ^{35}Cl resonance of an infinitely dilute solution of NaCl in H_2O. The ^{35}Cl chemical shift of solid NaCl with respect to aqueous NaCl is −45.37 ppm.[66]

Acknowledgements

Dr. Glenn Facey and Dr. Victor Terskikh are thanked for NMR spectrometer support and for helpful comments. We are grateful to Professor Tom Woo and Dr. Saman Alavi for access to computational resources and technical assistance with CASTEP. We thank members of the solid-state NMR group at the University of Ottawa for helpful discussions. Access to the 900 MHz NMR spectrometer was provided by the National Ultrahigh Field NMR Facility for Solids (Ottawa, Canada), a national research facility funded by the Canada Foundation for Innovation, the Ontario Innovation Trust, Recherche Québec, the National Research Council of Canada, and Bruker Biospin and managed by the University of Ottawa (www.nmr900.ca). The Natural Sciences and Engineering Research Council (NSERC) of Canada is acknowledged for a Major Resources Support grant. D.L.B. thanks NSERC for generous funding. E.B.B. thanks the University of Ottawa Faculty of Graduate and Postdoctoral Studies for a summer research scholarship.

[1] R. D. Goodenough, V. A. Stenger in *Comprehensive Inorganic Chemistry* (Eds.: J. C. Bailar, Jr., H. J. Emeléus, R. Nyholm, A. F. Trotman-Dickenson), Pergamon Press, Oxford, **1973**, Chapter 10.

[2] C. H. Christensen, R. Z. Sørensen, T. Johannessen, U. J. Quaade, K. Honkala, T. D. Elmøe, R. Køhler, J. K. Nørskov, *J. Mater. Chem.* **2005**, *15*, 4106–4108.

[3] C. H. Christensen, T. Johannessen, R. Z. Sørensen, J. K. Nørskov, *Catal. Today* **2006**, *111*, 140–144.

[4] J. S. Hummelshøj, R. Z. Sørensen, M. Y. Kustova, T. Johannessen, J. K. Nørskov, C. H. Christensen, *J. Am. Chem. Soc.* **2006**, *128*, 16–17.

[5] H. Kimura, J. Kai, *Energy Convers. Manage.* **1988**, *28*, 197–200.

[6] J. Chen, M. Yoshida, Y. Maekawa, N. Tsubokawa, *Polymer* **2001**, *42*, 9361–9365.

[7] G. Sberveglieri, G. Faglia, R. Ricci, R. Murri, N. Pinto, *Sens. Actuators B* **1993**, *13–14*, 615–616.

[8] D. L. Bryce, G. D. Sward, *Magn. Reson. Chem.* **2006**, *44*, 409–450.
[9] M. E. Smith, *Annu. Rep. NMR Spectrosc.* **2001**, *43*, 121–175.
[10] R. K. Harris, *Analyst* **2006**, *131*, 351–373.
[11] D. L. Bryce, K. Eichele, R. E. Wasylishen, *Inorg. Chem.* **2003**, *42*, 5085–5096.
[12] D. C. Apperley, R. A. Fletton, R. K. Harris, R. W. Lancaster, S. Tavener, T. L. Threlfall, *J. Pharm. Sci.* **1999**, *88*, 1275–1280.
[13] S. E. Ashbrook, L. Le Pollès, R. Gautier, C. J. Pickard, R. I. Walton, *Phys. Chem. Chem. Phys.* **2006**, *8*, 3423–3431.
[14] R. K. Harris in *Encyclopedia of Nuclear Magnetic Resonance* (Eds.: D. M. Grant, R. K. Harris), Wiley, Chichester, **1996**, pp. 3734–3740.
[15] T. O. Sandland, L.-S. Du, J. F. Stebbins, J. D. Webster, *Geochim. Cosmochim. Acta* **2004**, *68*, 5059–5069.
[16] J. F. Stebbins, L.-S. Du, *Am. Mineral.* **2002**, *87*, 359–363.
[17] K. Saito, K. Kanehashi, I. Komaki, *Annu. Rep. NMR Spectrosc.* **2001**, *44*, 23–74.
[18] F. Barberon, V. Baroghel-Bouny, H. Zanni, B. Bresson, J.-B. d'Espinose de la Caillerie, L. Malosse, Z. Gan, *Magn. Reson. Imaging* **2005**, *23*, 267–272.
[19] H. Yun, M. E. Patton, J. H. Garrett Jr. , G. K. Fedder, K. M. Frederick, J.-J. Hsu, I. J. Lowe, I. J. Oppenheim, P. J. Sides, *Cem. Concr. Res.* **2004**, *34*, 379–390.
[20] O. M. Jensen, M. S. H. Korzen, H. J. Jakobsen, J. Skibsted, *Adv. Cement. Res.* **2000**, *12*, 57–64.
[21] M. D. Andersen, H. J. Jakobsen, J. Skibsted, *J. Phys. Chem. A* **2002**, *106*, 6676–6682.
[22] J. Skibsted, M. D. Andersen, H. J. Jakobsen, Poster Presentation, *43rd Rocky Mountain Conference on Analytical Chemistry, NMR Symposium*, Denver, Colorado (USA), **2001**.
[23] J. Skibsted, H. J. Jakobsen, *Inorg. Chem.* **1999**, *38*, 1806–1813.
[24] F. Lefebvre, *J. Chim. Phys.* **1992**, *89*, 1767–1777.
[25] D. L. Bryce, G. D. Sward, S. Adiga, *J. Am. Chem. Soc.* **2006**, *128*, 2121–2134.
[26] D. L. Bryce, G. D. Sward, *J. Phys. Chem. B* **2006**, *110*, 26461–26470.
[27] M. D. Segall, P. J. D. Lindan, M. J. Probert, C. J. Pickard, P. J. Hasnip, S. J. Clark, M. C. Payne, *J. Phys. Condens. Matter* **2002**, *14*, 2717–2744.
[28] C. J. Pickard, F. Mauri, *Phys. Rev. B* **2001**, *63*, 245101.
[29] M. Profeta, F. Mauri, C. J. Pickard, *J. Am. Chem. Soc.* **2003**, *125*, 541–548.
[30] C. J. Pickard, F. Mauri in *Calculation of NMR and EPR Parameters. Theory and Applications* (Eds.: M. Kaupp, M. Bühl, V. G. Malkin), Wiley-VCH, Weinheim, **2004**, Chapter 16.
[31] M. Benoit, M. Profeta, F. Mauri, C. J. Pickard, M. E. Tuckerman, *J. Phys. Chem. B* **2005**, *109*, 6052–6060.
[32] R. K. Harris, S. A. Joyce, C. J. Pickard, S. Cadars, L. Emsley, *Phys. Chem. Chem. Phys.* **2006**, *8*, 137–143.
[33] N. Mifsud, B. Elena, C. J. Pickard, A. Lesage, L. Emsley, *Phys. Chem. Chem. Phys.* **2006**, *8*, 3418–3422.
[34] R. T. Hart, J. W. Zwanziger, U. Werner-Zwanziger, J. R. Yates, *J. Phys. Chem. A* **2005**, *109*, 7636–7641.
[35] J. W. Zwanziger, U. Werner-Zwanziger, J. L. Shaw, C. So, *Solid State Nucl. Magn. Reson.* **2006**, *29*, 113–118.
[36] J. W. Zwanziger, U. Werner-Zwanziger, E. D. Zanotto, E. Rotari, L. N. Glebova, L. B. Glebov, J. F. Schneider, *J. Appl. Phys.* **2006**, *99*, 083511.
[37] J. W. Zwanziger, J. L. Shaw, U. Werner-Zwanziger, B. G. Aitken, *J. Phys. Chem. B* **2006**, *110*, 20123–20128.
[38] J. V. Hanna, K. J. Pike, E. R. Vance, M. E. Smith, *Poster presentation at the 48th Rocky Mountain Conference on Analytical Chemistry (NMR Symposium)*, Breckenridge, Colorado (USA), **2006**.
[39] A. T. Jensen, *Struct. Rep.* **1942–1944**, *9*, 161–162.
[40] H. Honda, *Z. Naturforsch.* **2003**, *58a*, 623–630.
[41] P. Pyykkö, *Mol. Phys.* **2001**, *99*, 1617–1629.
[42] R. B. English, L. R. Nassimbeni, *Acta Crystallogr. Sect. C* **1984**, *40*, 580–581.
[43] I. Abrahams, E. Vordemvenne, *Acta Crystallogr. Sect. C* **1995**, *51*, 183–185.
[44] G. C. Campbell, R. C. Crosby, J. F. Haw, *J. Magn. Reson.* **1986**, *69*, 191–195.
[45] A.-R. Grimmer, A. Kretschmer, V. B. Cajipe, *Magn. Reson. Chem.* **1997**, *35*, 86–90.
[46] L. C. M. van Gorkom, J. M. Hook, M. B. Logan, J. V. Hanna, R. E. Wasylishen, *Magn. Reson. Chem.* **1995**, *33*, 791–795.
[47] B. Langer, I. Schnell, H. W. Spiess, A.-R. Grimmer, *J. Magn. Reson.* **1999**, *138*, 182–186.
[48] M. Xu, K. D. M. Harris, *J. Am. Chem. Soc.* **2005**, *127*, 10832–10833.
[49] G. M. Bowers, K. T. Mueller, *Phys. Rev. B* **2005**, *71*, 224112.
[50] X. Hou, R. J. Kirkpatrick, *Chem. Mater.* **2002**, *14*, 1195–1200.
[51] V. M. Padmanabhan, V. S. Jakkal, J. Shankar, *Indian J. Pure. Appl. Phys.* **1963**, *1*, 293–295.
[52] E. B. Brackett, T. E. Brackett, R. L. Sass, *J. Phys. Chem.* **1963**, *67*, 2132–2135.
[53] C. Gervais, R. Dupree, K. J. Pike, C. Bonhomme, M. Profeta, C. J. Pickard, F. Mauri, *J. Phys. Chem. A* **2005**, *109*, 6960–6969.
[54] T. T. Basiev, N. I. Batyrev, V. V. Voronov, V. A. Konyushkin, S. V. Kuznetsov, V. V. Osiko, A. M. Samartsev, E. B. Samoilova, P. P. Fedorov, *Russ. J. Appl. Chem.* **2005**, *78*, 1035–1037. (Translated from *Zh. Prikladnoi Khimii* **2005**, *78*, 1057–1059.)
[55] T. L. Weeding, W. S. Veeman, *J. Chem. Soc. Chem. Commun.* **1989**, 946–948.
[56] a) R. Siegel, T. T. Nakashima, R. E. Wasylishen, *Chem. Phys. Lett.* **2004**, *388*, 441–445; b) R. Siegel, T. T. Nakashima, R. E. Wasylishen, *Concepts Magn. Reson.* **2005**, *26A*, 47–61.
[57] a) H. Y. Carr, E. M. Purcell, *Phys. Rev.* **1954**, *94*, 630–638; b) S. Meiboom, D. Gill, *Rev. Sci. Instrum.* **1958**, *29*, 688–691.
[58] J. T. Cheng, P. D. Ellis, *J. Phys. Chem.* **1989**, *93*, 2549–2555.
[59] F. H. Larsen, H. J. Jakobsen, P. D. Ellis, N. C. Nielsen, *J. Phys. Chem. A* **1997**, *101*, 8597–8606.
[60] W. P. Power, R. E. Wasylishen, S. Mooibroek, B. A. Pettitt, W. Danchura, *J. Phys. Chem.* **1990**, *94*, 591–598.
[61] K. Eichele, R. E. Wasylishen, *WSOLIDS NMR Simulation Package*, *Version 1.17.30*, Universitat Tübingen, Tübingen (Germany), **2001**.
[62] D. Massiot, F. Fayon, M. Capron, I. King, S. Le Calvé, B. Alonso, J.-O. Durand, B. Bujoli, Z. Gan, G. Hoatson, *Magn. Reson. Chem.* **2002**, *40*, 70–76.
[63] J. Mason, *Solid State Nucl. Magn. Reson.* **1993**, *2*, 285–288.
[64] a) J. P. Perdew, K. Burke, M. Ernzerhof, *Phys. Rev. Lett.* **1996**, *77*, 3865–3868; b) J. P. Perdew, K. Burke, M. Ernzerhof, *Phys. Rev. Lett.* **1997**, *78*, 1396.
[65] M. Gee, R. E. Wasylishen, A. Laaksonen, *J. Phys. Chem. A* **1999**, *103*, 10805–10812.
[66] D. L. Bryce, M. Gee, R. E. Wasylishen, *J. Phys. Chem. A* **2001**, *105*, 10413–10421.
[67] K. Brandenburg, *Diamond 3.0e*, **1997–2005**, Crystal Impact GbR, Bonn (Germany).
[68] C. Cason, *POV-Ray for Windows*, Version 3.6.1a.icl8.win32, **2004**.
[69] P. A. Agron, W. R. Busing, *Acta Crystallogr. Sect. C* **1985**, *41*, 8–10.
[70] A. Leclaire, M. M. Borel, *Acta Crystallogr. Sect. B* **1977**, *33*, 1608–1610.
[71] H. Ott, *Z. Kristallogr. Kristallgeom. Kristallphys. Kristallchem.* **1926**, *63*, 222–230.
[72] H. Möller, H. D. Lutz, *Acta Crystallogr. Sect. C* **1993**, *49*, 944–946.
[73] P. A. Agron, W. R. Busing, *Acta Crystallogr. Sect. C* **1986**, *42*, 141–143.
[74] V. M. Padmanabhan, W. R. Busing, H. A. Levy, *Acta Crystallogr.* **1963**, *16*, A26.
[75] V. M. Padmanabhan, W. R. Busing, H. A. Levy, *Acta Crystallogr. Sect. B* **1978**, *34*, 2290–2292.

Received: January 12, 2007
Published online: March 23, 2007

